Microstructural properties of $Bi_2Sr_2Ca_{n-1}Cu_nO_y$ multilayers grown by molecular beam epitaxy

A. Vailionis, A. Brazdeikis, and A. S. Flodström
Materials Physics, Department of Physics, Royal Institute of Technology, S-100 44 Stockholm, Sweden
(Received 6 August 1996)

The microstructure of $Bi_2Sr_2Ca_{n-1}Cu_nO_y$ multilayers grown by molecular beam epitaxy on atomically flat $SrTiO_3$ substrates has been studied by reflection high-energy electron diffraction (RHEED), atomic force microscopy, and x-ray-diffraction (XRD) techniques. The overall RHEED data, collected *in situ* at different $Bi_2Sr_2CuO_y/Bi_2Sr_2CaCu_2O_y$ (2201/2212) multilayer growth stages, demonstrated a two-dimensional growth and rather a high quality of the interfaces. Following the evolution of RHEED patterns, some evidence of an increase in surface roughness after several multilayer periods, was detected. A one-dimensional x-ray-diffraction model was applied for a quantitative analysis of growth defects in the multilayers. The substitutional disorder in the lattice and stacking faults in the molecular layers were determined by an iterative comparison of simulated x-ray-diffraction spectra with the experimental XRD data. The observed changes in the c-axis lattice parameter of 2201 molecular layers were interpreted as being caused by ionic substitutions of Sr^{2+} by Ca^{2+} in the lattice and governed by the growth interdiffusion. The fitting procedure also revealed that two types of growth disorder were present in the layers: (1) stacking faults randomly distributed within the layers and (2) stacking faults localized at the interfaces. The two types of growth defect are expected to influence the superconducting properties differently and this has to be considered before the transport properties of superconducting multilayers are studied. [S0163-1829(96)10145-4]

INTRODUCTION

Multilayers of conventional superconductors have been extensively studied both for fundamental research and for device applications. The artificially layered structures exhibit a number of interesting effects such as a dimensional crossover and the proximity effect.[1–5] Multilayers of high-temperature superconductors (HTS's) offer further possibilities of studying these and also other effects, such as the Kosterlitz-Thouless transition and the electric-field effect.[6–8] Various film synthesis techniques have so far been employed for the fabrication of superconducting multilayers, of which the most common are magnetron sputtering,[9,10] laser ablation,[11] and molecular beam epitaxy (MBE).[12] These advanced techniques, especially MBE, provide the opportunity of producing high-quality multilayers, but the complexity of the crystal structure and the multielement nature of the high-T_c cuprates makes reproducible preparation rather a difficult task. The $Bi_2Sr_2Ca_{n-1}Cu_nO_y$ compounds are very suitable for fabricating HTS multilayers for many device applications and also as layered model systems for growth studies, due to the presence of several constituent phases exhibiting similar and lattice-matched crystal structures, and possessing different T_c values.[10,12]

It is known that the transport properties of HTS materials are sensitive to the overall structural quality and to the number of growth defects such as ionic substitutions, stacking faults, and oxygen stoichiometry.[13,14] Many of these imperfections are common defects in $Bi_2Sr_2Ca_{n-1}Cu_nO_y$ compounds. The cationic substitutions that are related to the unit-cell disorder can affect some interplanar distances in the lattice.[15] Stacking faults (SF) are often formed during film growth because of the very similar free energies of formation of the adjacent phases.[16,17] In multilayer structures, in addition, defects can occur at the interfaces. The interface quality is primarily dependent on the substrate nature and its surface quality and is affected by lattice misfit, interdiffusion, and in some cases the oxygen stoichiometry.[18–20]

Many techniques have been used for the structural analysis of bulk HTS materials. Only a few of them have so far been applied to the quantitative structural study of thin films. Transmission electron microscopy (TEM) is particularly useful in revealing details on a micrometer scale and down to an atomic scale. Due to its relatively small probing volume, however, this technique is not very suitable for obtaining average quantitative information about interfaces and the unit-cell structure of the entire film. Reflection high-energy electron diffraction (RHEED) is widely used for the *in situ* analysis of surface structure and morphology and growth orientations. Thin-film and substrate surfaces can also be successfully studied by scanning probe techniques such as scanning tunneling microscopy (STM) and atomic force microscopy (AFM) and these techniques can provide quantitative data about the surface roughness. Both RHEED and scanning probe techniques are surface sensitive and it is therefore a complicated procedure to extract knowledge about intergrowth defects. X-ray-diffraction is a nondestructive method for structural analysis and it provides useful information about film microstructure and, because of its large penetration depth, it can also provide average structural data. A combination of these techniques exhibiting different resolutions can be a powerful tool for the quantitative microstructural analysis of complex oxide films and multilayers. Most structural studies have so far been performed on the $YBa_2Cu_3O_{7-\delta}/RBa_2Cu_3O_{7-\delta}$ (R=rare earth) superconducting multilayers where the microstructural quality was studied by transmission electron microscopy,[18–21] x-ray diffraction (XRD)[22,23] and atomic force microscopy.[22,24] There is a lack of quantitative structural data for Bi-based superconducting multilayers, although the physical properties have been ex-

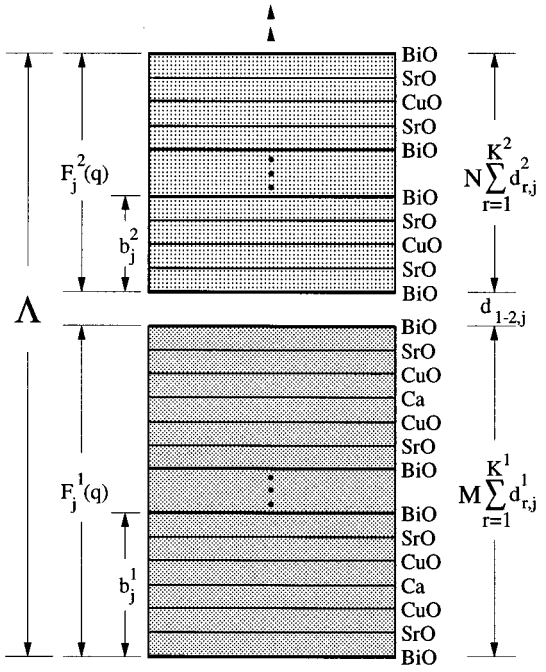

FIG. 1. A schematic model of a 2201/2212 multilayer. Each bilayer contains *M* and *N* molecular units of 2212 and 2201 stuctures, respectively. Each molecular unit consists of a certain number of BiO, SrO, CuO, and Ca planes. $F_j^1(q)$, b_j^1 and $F_j^2(q)$, b_j^2 are the structure factors and BiO-BiO distances of 2212 and 2201 molecular units, respectively.

tensively studied.[10,25,26] To fill in this gap, detailed microstructural investigations combining several complementary analysis techniques are necessary.

In the present study, the microstructure of MBE-grown $Bi_2Sr_2CuO_y/Bi_2Sr_2CaCu_2O_y$ (2201/2212) multilayers has been analyzed by a combination of RHEED, AFM, and XRD techniques. A one-dimensional kinematic x-ray-diffraction model was applied to obtain quantitative information about the structural quality of the multilayers. A unit-cell disorder as well as growth defects in individual 2201 and 2212 layers were observed. Two different types of growth disorder were resolved: (1) stacking faults randomly distributed in the layers and (2) stacking faults localized at the interfaces.

EXPERIMENTAL

The experiments were conducted in a combined MBE/AFM/STM system, custom designed for the study of growth mechanisms, interfaces, and surfaces of complex metal oxide films and HTS-related materials.[27,28] Superconducting multilayers were grown using a layer-controlled MBE technique on UHV-annealed and well-characterized $SrTiO_3$ (100) substrates. Molecular beams of Bi, Sr, Ca, and Cu were provided from Knudsen-type effusion cells using high purity metals. *In situ* oxidation of the deposited species at the substrate temperatures of 650–720 °C was achieved using nitrogen dioxide, NO_2, gas. Prior to the growth, the quality of the substrate surface was examined by an AFM operating in a contact mode and using Si_3N_4 cantilevers with a typical tip radius of 20 nm. During the growth, the evolution of interface structure and morphology was monitored *in situ* by a 15 keV RHEED. More detailed information concerning the combined MBE/AFM/STM system, the substrate surfaces, and their preparation conditions can be found elsewhere.[27–29]

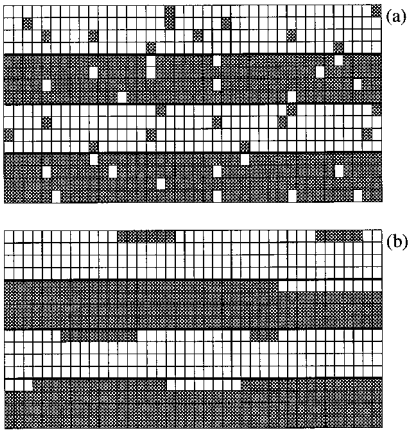

FIG. 2. Schematic representations of a 2201/2212 multilayer containing growth defects of (a) randomly distributed stacking faults and (b) stacking faults localized at the interfaces (interface roughness).

After the multilayer growth, their microstructure was studied by XRD. The experimental data were collected utilizing an x-ray powder diffractometer in the Bragg-Brentano geometry using Cu $K\alpha$ radiation ($\lambda = 1.5406$ Å) and equipped with a graphite monochromator for a diffracted beam. The data were further used for a quantitative microstructural analysis of these multilayers by the application of a one-dimensional kinematic x-ray-diffraction model.[30] A detailed mathematical formalism of the model developed for thin $Bi_2Sr_2Ca_{n-1}Cu_nO_y$ films and multilayers has been published elsewhere.[15,31] For the structure factor calculations, a model structure of a $Bi_2Sr_2CuO_y/Bi_2Sr_2CaCu_2O_y$ multilayer (shown in Fig. 1) has been used. The multilayer consists of *N* molecular units of 2201 and *M* molecular units of 2212 assembled in the direction perpendicular to the substrate surface. Each molecular unit considered represents *one half of the unit cell of the corresponding bulk phase*. All corrections such as the Debye-Waller coefficient, Lorentz-polarization, and absorption factors were considered. The calculated x-ray-diffraction profiles were compared with the measured XRD spectra using the following fitting parameters: interplanar distances and site occupancies in the unit cell, and the number of stacking faults in a layer. Two different types of growth disorder as shown in Figs. 2(a) and 2(b) were considered: (1) stacking faults randomly distributed within layers and (2) stacking faults localized at the interfaces. The growth disorder is considered to be a discrete disorder resulting from different crystalline structures.[32] The interplanar distances, $d_{r,j}$, as shown in Fig. 1 are assumed to vary continuously around some average d_r value according to the Gaussian distribution function.

RESULTS AND DISCUSSION

Typical $SrTiO_3$ (100) surfaces prepared by annealing in an UHV displayed regular arrays of 0.4 nm steps spaced by flat terraces of about 100–400 nm. Such surfaces and the

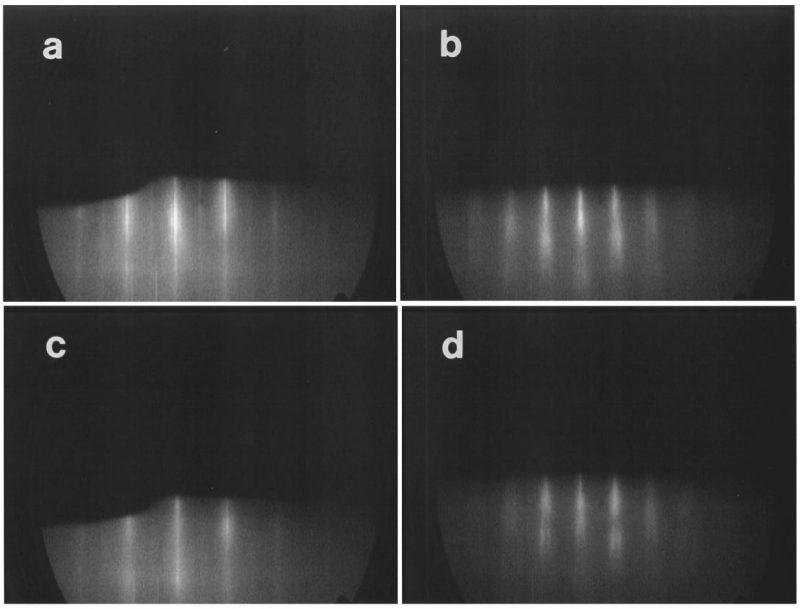

FIG. 3. *In situ* recorded RHEED patterns of resulting 2201-2212 and 2212-2201 interfaces of a $2201_3/2212_4$ multilayer. Patterns (a) and (b) were recorded after the growth of three molecular layers of 2201 on $SrTiO_3$. Patterns (c) and (d) were recorded after the growth of the next four molecular layers of 2212. The images (a), (c) were taken along the [100] and (b), (d) along the [110] azimuths of $SrTiO_3$.

corresponding RHEED patterns obtained were very similar to those already published elsewhere.[29] Each 2201/2212 multilayer growth began with the predeposition of Sr monolayer followed by Cu and Sr, thus resulting in abrupt interfaces between the $SrTiO_3$ (100) surfaces and the first 2201 molecular layers. Figure 3 shows RHEED patterns of the resulting 2201-2212 and 2212-2201 interfaces of a $2201_3/2212_4$ multilayer recorded *in situ* after the growth of three molecular units of 2201 [(a) and (b)] and the further growth of the next four molecular units of 2212 [(c) and (d)]. The (a) and (c) images were taken along [100], and (b) and (d) along the [110] $SrTiO_3$ azimuths. The two-dimensional (2D) RHEED patterns obtained suggest that the multilayer growth on $SrTiO_3$ (100) surfaces occurs in the form of large 2D islands. In addition, many 2201 and 2212 bulk features such as the incommensurate modulations and the presence of 90°-oriented twist domains are clearly resolved by RHEED. These features are visible as the satellite reflections surrounding the main reciprocal-lattice rods [Figs. 3(a) and 3(c)] and also as the prominent splitting (Λ form) of the lattice rods [Figs. 3(b) and 3(d)]. The overall RHEED data indicate a rather high quality of the interfaces. An intensity distribution visible along the fundamental reflections, especially in the case of the 2212 surface, indicates however that there is some degree of interface roughness. The interface roughness is observed to increase after several multilayer periods, although no significant changes from 2D RHEED patterns were obtained.

A low-angle XRD spectrum of a $2201_3/2212_4$ multilayer is presented in Fig. 4. Eminent fringe-type oscillations (Kiessig fringes) which are rather high in amplitude, and the Bragg diffraction peaks corresponding to 2201, 2212, and 2201/2212 structures are clearly visible. These interference oscillations occur when coherent and parallel x-ray waves interfere if they are diffracted from atomic layers and well-defined interfaces. Experimental low-angle XRD data indicate that a periodic chemical modulation in 2201/2212 multilayers is evidently maintained. The estimated (from fringe spacing, $\Delta\theta$) total multilayer thickness was in a good agreement with the growth design of the corresponding individual 2201 and 2212 molecular layers.

The calculated high-angle x-ray diffraction profile of a perfect $(2201_3/2212_4)_4$ multilayer is shown in Fig. 5(a). Although the simulated spectra have the same qualitative features as the measured profile [Fig. 5(b)], some discrepancies in the linewidths and in the relative intensities of main and satellite peaks can be observed. The measured XRD profiles exhibit somewhat lower peak intensities and broader linewidths. Such features can only be explained by a reduced crystalline order in the multilayer due to structural imperfections in the film.

Figures 6(a) and 6(b) represent the calculated intensities and linewidths of the fourth and sixth multilayer peaks as a function of a discrete disorder. Evidently both stacking faults and interface roughness affect the shape of the peaks. The intensities and the linewidths are found, however, to be more sensitive to the randomly populated SF than to that localized at the interfaces. The shapes of the satellite peaks are also found to be affected in a similar manner. The observed fea-

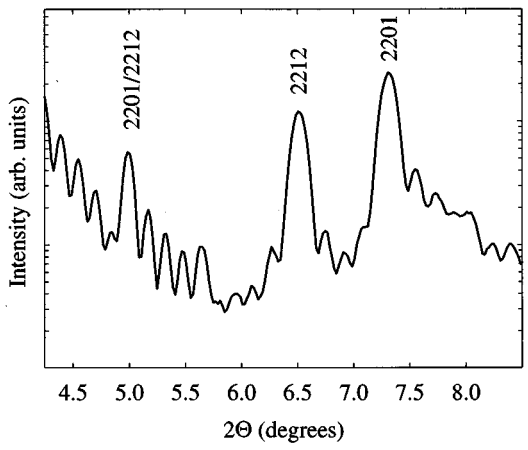

FIG. 4. Low-angle XRD spectrum of a $(2201_3/2212_4)_4$ multilayer. The Kiessig-type fringes and Bragg peaks corresponding to the 2201, 2212, and 2201/2212 periods are visible.

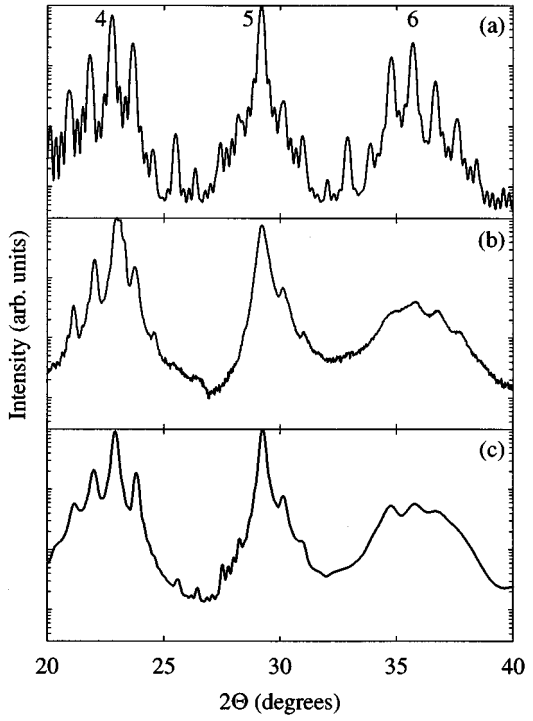

FIG. 5. High-angle x-ray-diffraction spectra of a $(2201_3/2212_4)_4$ multilayer: (a) calculated spectrum of a perfect multilayer, (b) measured data, and (c) refined spectrum.

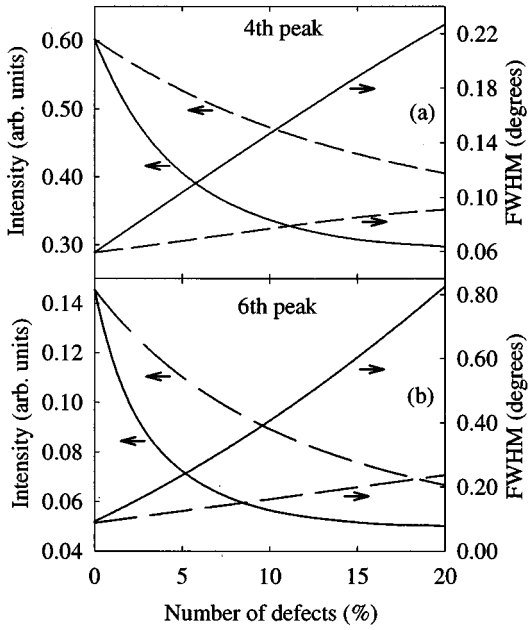

FIG. 6. Calculated intensity and FWHM of (a) the fourth and (b) the sixth main peaks of a $(2201_4/2212_4)_{15}$ multilayer as a function of the discrete disorder. The solid line indicates randomly distributed stacking faults, and the dashed line indicates stacking faults localized at the interfaces (interface roughness). The intensities are normalized to the fifth peak intensity.

tures can be explained as being due to a suppression of the long-range crystalline order (coherence) either at the interfaces or in the layers when SF are created and these features can apparently be used for studying these defects in thin films. The sensitivity is large enough to distinguish the stacking faults from the interface roughness for 2201/2212 multilayers with $M, N \geqslant 2$. It can be understood from Fig. 2(b), that there are limitations for multilayers with $M, N=1$, where any layer thickness fluctuation of the order of one molecular unit of 2201 or 2212 is considered to be adequate to SF in the layers.

Calculations also revealed that the satellite peak intensities surrounding the fifth multilayer peak of the 2201/2212 multilayer (Fig. 7) are very sensitive to the c-axis parameter value of the constituent molecular units. The simulated x-ray-diffraction profile exhibits rather a large suppression of these satellite peaks when the c-axis lattice parameter is considered to be either contracted for the 2201 molecular unit or expanded for the 2212 unit, compared to the corresponding parameters of the bulk compounds. This is demonstrated in the case of the $(2201_3/2212_4)_{10}$ multilayer in Figs. 7(b) and 7(c) where the 2201 molecular unit is contracted from 24.62 to 24.3 Å and the 2212 molecular unit is expanded from 30.87 to 31.27 Å, respectively. In addition to this suppression, a change in the c-axis parameter also induces a shift of the XRD peaks: (1) towards higher angles when the 2201 molecular unit is considered to be contracted and (2) towards lower angles when the 2212 molecular unit is considered to be expanded, according to the following relation:

$$\frac{2\sin\theta}{\lambda} = \frac{1}{d} \pm \frac{n}{\Lambda}, \tag{1}$$

where λ is the wavelength of x rays (1.5406 Å), θ is the Bragg angle, and n is the order of the satellite peak surrounding the main peak. The d value for a 2201/2212 multilayer is given by

$$d = \left(N \frac{c_{2201}}{l_{2201}} + M \frac{c_{2212}}{l_{2212}} \right) \Big/ (N+M), \tag{2}$$

where c_{2201}, l_{2201} and c_{2212}, l_{2212} are the c-axis lengths and the Miller indices of 2201 and 2212 molecular units, respectively.

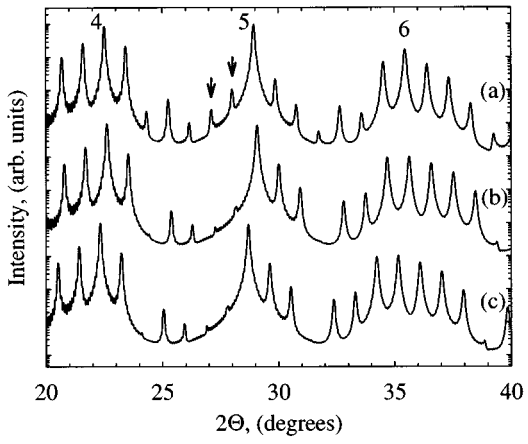

FIG. 7. Calculated x-ray-diffraction profile of a $(2201_3/2212_4)_{10}$ multilayer. The c-axis lattice parameters of 2201 and 2212 molecular units were considered to be (a) 24.62 and 30.87 Å, (b) 24.3 and 30.87 Å, and (c) 24.62 and 31.27 Å, respectively.

TABLE I. Refined parameters for selected 2201/2212 multilayers. Number of defects (stacking faults and interface roughness) corresponds to the number of molecular units of adjacent phases distributed within the layer per unit volume.

	2201 layers				2212 layers				
						Number of integrowth defects (%)			
Sample 2201/2212	Unit-cell length (Å)	Number of integrowth defects (%)	Number of defects related to the surface roughness (%)	Interface roughness at the 2201-2212 interface[a] (%)	Unit-cell length (Å)	2201	2223	Number of defects related to the surface roughness (%)	Interface roughness at the 2212-2201 interface[a] (%)
3/4×4	24.41	0	15	15	30.87	3	17	15	35
2/2×9	24.38	0	18	18	30.87	6	22	18	46
1/3×15	24.40		20		30.87	5	21	20	46

[a]The interface roughness represents a sum of intergrowth defects within the corresponding layer and defects related to the surface roughness.

A fitted x-ray-diffraction profile of the $(2201_3/2212_4)_4$ multilayer is shown in Figs. 5(c). Both peak intensities and linewidths are reproduced rather well. The refined c-axis lattice parameters, the type and the number of defects in some 2201/2212 multilayers are listed in Table I. The fitting procedure revealed that, for most of the multilayers investigated here, the average c-axis lattice parameter of the 2201 molecular unit is somewhat smaller than that of the 2201 bulk compound. It is suggested that this feature is possibly related to the Sr^{2+} substitutions by Ca^{2+} ions in the lattice, since similar results were observed for MBE-grown 2212 films.[15] Such substitutional disorder does affect an average 2212 lattice by expansion of the Ca-CuO and contraction of the SrO-CuO interplanar distances, while the c-axis lattice parameter remains unchanged. In the case of a 2201 layer, as can be seen in Fig. 1, the BiO-SrO and the SrO-CuO distances define the lattice in the c-axis direction and any change in the occupational parameter of the Sr site should thus affect the c-axis length.

It is expected that the substitutions of Sr^{2+} ions by Ca^{2+} resolved in the 2201 layers are governed by the growth interdiffusion, which is rather high at these elevated substrate temperatures. In the case of layer-controlled growth, interdiffusion is undesirable because the growth kinetics are expected to dominate over the thermodynamics.[33] The interdiffusion rate seems to be much lower than the rate of the surface diffusion, as epitaxial film growth is evidently achieved, and the designed multilayer structure is maintained. Another factor which can cause changes in the c-axis lattice parameter is related to the oxidation level of 2201.[34] This possibility is however discarded because the same oxidation conditions were maintained during the growth for both 2201 and 2212 layers and the measured 2212 layer c-axis lattice parameter was unchanged.

The linewidth of high-angle XRD peaks resulting from a $Bi_2Sr_2Ca_{n-1}Cu_nO_y$ structure can be affected by the presence of intergrowth defects, mainly of adjacent phases randomly created within the layers. These defects occur because of the very similar thermodynamic free energies of the adjacent polytype phases and, in the case of MBE-grown 2212 films, it has been discussed in detail elsewhere.[17] The probability of stacking fault formation is rather high in 2212 layers and much lower in 2201 layers, because 2201 is one of the most stable phases among other polytypes (2212 and 2223).

XRD modeling also suggested that there would be a nonuniform distribution of stacking faults within the sequentially assembled molecular layers. As can be seen in Table I, more intergrowth defects were localized at the interfaces than were observed within the layers. The stacking faults at the interfaces can simply be attributed to the increase in interface roughness. Its origin is probably related both to local variations in stoichiometry of the growth surface and to the layer surface roughness itself. It has been already demonstrated that local nonstoichiometry leads to stacking faults of adjacent phases in 2212.[17] The surface roughness is related to the so-called ''half-unit-cell-by-half-unit-cell'' growth mode of both 2201 and 2212, which has been previously discussed by other authors on the basis of RHEED and STM studies.[35–37] The present result is in good agreement with the earlier RHEED observations, predicting an increase in 2201-2212 and 2212-2201 interface roughness after the growth of several multilayer periods.

In addition, a disorder related to the continuous fluctuations in interplanar distances of 2201 and 2212 molecular units was observed. This structural imperfection occurs because of the random scatter of interplane distances $d_{r,j}$ around the average d_r values caused by local imperfections. These fluctuations, however, appeared to be no greater than 0.06 Å.

It is known that stacking faults affect a superconducting transition of Bi-based superconducting cuprates.[16,38] Typical T_c values of the 2212 phase are about 85 K, while that for the 2201 phase are typically lower than 20 K. As can be seen in Fig. 2(a), the presence of 2201 structures in 2212 layers as randomly populated stacking faults can have a significant effect on the current flow. This type of defect is expected to affect a superconducting transition. A more favorable situation occurs when the SF are localized only at the interfaces, as shown in Fig. 2(b), since the rest of the 2212 layers still maintain a defect-free structure. In this case, the current flow in the (ab) plane may not interfere with the low-T_c 2201 phase, and such 2201/2212 multilayers are expected to exhibit the intrinsic transport properties of the 2212 phase, but with a reduced layer thickness. Further experiments with 2201/2212 superconducting multilayers in relation to this interpretation are presently in progress.

CONCLUSIONS

The microstructure of 2201/2212 multilayers grown on atomically flat substrates by MBE was studied using

RHEED, AFM, and XRD techniques. *In situ* RHEED images revealed a two-dimensional growth and a slightly increase in interface roughness as the growth proceeded. A one-dimensional kinematic x-ray-diffraction model was applied to provide a quantitative analysis of the growth defects in the superconducting multilayers. The disorder both in the unit cell and in the layers was determined by an iterative fitting of a simulated x-ray-diffraction profile to the measured XRD spectra. The observed shorter c-axis lattice parameter of 2201 molecular layers is interpreted as being caused by ionic substitutions governed by the growth interdiffusion. Two types of growth disorder were resolved in 2201/2212 multilayers: (1) stacking faults randomly distributed in the layers and (2) stacking faults localized at the interfaces (interface roughness). The observed larger concentration of stacking faults at the interfaces is attributed to the surface roughness of one molecular unit height distinct for the Bi-based films. The intergrowth defects in the layers and the interface roughness are expected to influence the multilayer superconducting properties in different way and, this must be taken into consideration when transport properties are interpreted.

ACKNOWLEDGMENTS

This work was supported by the Swedish Research Council for Engineering Sciences (TFR) and the Swedish National Board for Industrial and Technical Development (NUTEK).

[1] I. Banerjee, Q. S. Yang, C. M. Falco, and I. K. Schuller, Phys. Rev. B **28**, 5037 (1983).
[2] P. R. Broussard and T. H. Geballe, Phys. Rev. B **35**, 1664 (1987).
[3] Q. S. Yang, C. M. Falco, and I. K. Schuller, Phys. Rev. B **27**, 3867 (1983).
[4] W. P. Lowe and T. H. Geballe, Phys. Rev. B **29**, 4961 (1984).
[5] J.-M. Triscone, D. Ariosa, M. G. Karkut, and Ø. Fischer, Phys. Rev. B **35**, 3238 (1987).
[6] J. Z. Wu, C. S. Ting, W. K. Chu, and X. X. Yao, Phys. Rev. B **44**, 411 (1991).
[7] M. Rasolt, T. Edis, and Z. Tešanović, Phys. Rev. Lett. **66**, 2927 (1991).
[8] S. Sakai, Phys. Rev. B **47**, 9042 (1993).
[9] O. Nakamura, E. E. Fullerton, J. Guimpel, and I. K. Schuller, Appl. Phys. Lett. **60**, 120 (1992).
[10] T. Matsushima, Y. Ichikawa, H. Adachi, K. Setsune, and K. Wasa, Solid State Commun. **76**, 1201 (1990).
[11] D. H. Lowndes, D. P. Norton, and J. D. Budai, Phys. Rev. Lett. **65**, 1160 (1990).
[12] I. Bozovic, J. N. Eckstein, M. E. Klausmeier-Brown, and G. Virshup, J. Supercond. **5**, 19 (1992).
[13] J. L. MacManus-Driscoll, J. A. Alonso, P. C. Wang, T. H. Geballe, and J. C. Bravman, Physica C **232**, 288 (1994).
[14] A. Bertinotti, D. Colson, J. Hammann, J-F. Marucco, D. Luzet, A. Pinatel, and V. Viallet, Physica C **250**, 213 (1995).
[15] A. Vailionis, A. Brazdeikis, and A. S. Flodström, Phys. Rev. B **51**, 3097 (1995).
[16] J. M. Tarascon, W. R. McKinnon, P. Barboux, D. M. Hwang, B. G. Bagley, L. H. Greene, G. W. Hull, Y. LePage, N. Stoffel, and M. Giroud, Phys. Rev. B **38**, 8885 (1988).
[17] A. Brazdeikis, A. Vailionis, A. S. Flodström, and C. Træholt, Physica C **253**, 383 (1995).
[18] J.-M. Triscone, M. G. Karkut, L. Antognazza, O. Brunner, and Ø. Fischer, Phys. Rev. Lett. **63**, 1016 (1989).
[19] S. J. Pennycook, M. F. Chisholm, D. E. Jesson, D. P. Norton, D. H. Lowndes, R. Feenstra, H. R. Kerchner, and J. O. Thomson, Phys. Rev. Lett. **67**, 765 (1991).
[20] Qi Li, C. Kwon, S. Bhattacharya, C. Doughty, S. N. Mao, L. Senapati, X. X. Xi, T. Venkatesan, J. L. Peng, Z. Y. Li, R. L. Greene, K.-M. Ham, R. Sooryakumar, and S. A. Schwarz, Proc. SPIE **2157**, 142 (1994).
[21] D. P. Norton, D. H. Lowndes, S. J. Pennycook, and J. D. Budai, Phys. Rev. Lett. **67**, 1358 (1991).
[22] E. E. Fullerton, J. Guimpel, O. Nakamura, and I. K. Schuller, Phys. Rev. Lett. **69**, 2859 (1992).
[23] Ph. Lerch, F. Marcenat, Ph. Jacot, D. Ariosa, J. Perret, Ch. Leeman, P. Martinoli, M. Cantoni, and H. R. Ott, Physica C **242**, 30 (1995).
[24] J. P. Contour, C. Sant, D. Ravelosona, C. Dolin, J. Perrière, L. Ranno, P. Auvray, and J. Caulet, Appl. Surf. Sci. **75**, 252 (1994).
[25] M. Nakao, H. Furukawa, H. Mukaida, S. Fujiwara, and R. Yuasa, in *Advances in Superconductivity IV*, edited by H. Hayakawa and N. Koshizuka (Springer-Verlag, Tokyo, 1992), p. 797.
[26] A. Odagawa, K. Setsune, T. Matsushima, and T. Fujita, Phys. Rev. B **48**, 12 985 (1993).
[27] A. Brazdeikis, Licentiate thesis, Royal Institute of Technology, Stockholm, Sweden, 1994.
[28] A. Brazdeikis, A. Vailionis, and A. S. Flodström, J. Vac. Sci. Technol. (to be published).
[29] A. Brazdeikis and A. S. Flodström, Appl. Surf. Sci. (to be published).
[30] E. E. Fullerton, I. K. Schuller, H. Vanderstraeten, and Y. Bruynseraede, Phys. Rev. B **45**, 9292 (1992).
[31] A. Vailionis, Licentiate Thesis, Royal Institute of Technology, Stockholm, Sweden, 1996.
[32] J.-P. Locquet, D. Neerinck, L. Stockman, Y. Bruynseraede, and I. K. Schuller, Phys. Rev. B **39**, 13 338 (1989).
[33] I. Bozovic, J. N. Eckstein, G. F. Virshup, A. Chaiken, M. Wall, R. Howell, and M. Fluss, J. Supercond. **7**, 187 (1994).
[34] X. Z. Xu, M. Viret, H. Tebbji, and M. Laguës, Appl. Supercond. **1**, 755 (1993).
[35] T. Ishibashi, K. Song, Y. Okada, and M. Kawabe, Jpn. J. Appl. Phys. **31**, L406 (1992).
[36] S. Sakai, Y. Kasai, and P. Bodin, Jpn. J. Appl. Phys. **31**, L399 (1992).
[37] X. Zhu, G. C. Xiong, R. Liu, Y. J. Li, G. J. Lian, and Z. Z. Gan, J. Vac. Sci. Technol. B **12**, 2247 (1994).
[38] Y. Zhao, G. D. Gu, G. J. Russell, N. Nakamura, S. Tajima, J. G. Wen, K. Uehara, and N. Koshizuka, Phys. Rev. B **51**, 3134 (1995).